NeuroImage 207 (2020) 116428

Contents lists available at ScienceDirect

NeuroImage

journal homepage: www.elsevier.com/locate/neuroimage

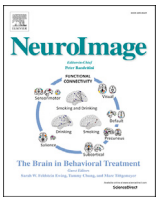

Higher resting-state BNST-CeA connectivity is associated with greater corrugator supercilii reactivity to negatively valenced images

Walker S. Pedersen *, Stacey M. Schaefer, Lauren K. Gresham, Seungbeum D. Lee, Michael P. Kelly, Jeanette A. Mumford, Jonathan A. Oler, Richard J. Davidson

university of wisconsin–madison, United States

A B S T R A C T

The bed nucleus of the stria terminalis (BNST) and central nucleus of the amygdala (CeA) are hypothesized to be the output nodes of the extended amygdala threat response, integrating multiple signals to coordinate the threat response via outputs to the hypothalamus and brainstem. The BNST and CeA are structurally and functionally connected, suggesting interactions between these regions may regulate how the response to provocation unfolds. However, the relationship between human BNST-CeA connectivity and the behavioral response to affective stimuli is little understood. To investigate whether individual differences in BNST-CeA connectivity are related to the affective response to negatively valenced stimuli, we tested relations between resting-state BNST-CeA connectivity and both facial electromyographic (EMG) activity of the corrugator supercilii muscle and eyeblink startle magnitude during affective image presentation within the Refresher sample of the Midlife in the United States (MIDUS) study. We found that higher right BNST-CeA connectivity was associated with greater corrugator activity to negative, but not positive, images. There was a trend-level association between right BNST-CeA connectivity and trait negative affect. Eyeblink startle magnitude was not significantly related to BNST-CeA connectivity. These results suggest that functional interactions between BNST and CeA contribute to the behavioral response to negative emotional events.

1. Introduction

The extended amygdala is a neuroanatomical macrostructure in the basal forebrain that plays a central role in responding to threat and generating negative emotional states (Davis, 1998; Fox et al., 2015; Heimer et al., 2007; Koob, 2008; Koob and Volkow, 2016). The central amygdala (CeA) and bed nucleus of the stria terminalis (BNST) serve as the output nodes for the extended amygdala threat response (Chrousos, 2009; Crane et al., 2003; Davis et al., 2010; Spencer et al., 2005). These regions help coordinate the autonomic and behavioral response to threat via projections to the hypothalamus and brainstem (Davis and Whalen, 2001). The BNST and CeA are structurally and functionally interconnected (Birn et al., 2014; Dong et al., 2001; Hofmann and Straube, 2019; Hofmann et al., 2012; Oler et al., 2012, 2017; Torrisi et al., 2015). The BNST receives gamma-aminobutyric acid (GABA) mediated innervation from the CeA (Dong et al., 2001). Many of these BNST-projecting fibers coming from the CeA also contain corticotropin-releasing factor (Sakanaka, et al. 1986), which Davis et al. (2010) proposed drives the BNST response to sustained threat. This is consistent with research suggesting that disruption of BNST-CeA connectivity reduces anxiety-like behaviors during a plus maze task (Cai et al., 2012). BNST projections to the CeA are also largely mediated by GABA (Gungor and Paré, 2016), and these connections appear to exert tonic inhibition on the CeA (Davis et al., 2010; Meloni et al., 2006). As such, the level of inhibition the BNST exerts on the CeA may regulate the threat response by determining the excitability of the CeA. Given this pattern of connectivity, interactions between the CeA and BNST likely play an important role in regulating the threat response.

While the BNST exhibits resting-state connectivity with the CeA (Oler et al., 2012; Torrisi et al., 2015), and BNST-CeA connectivity is associated with anxiety in nonhuman primates (Fox et al., 2018), the functional significance of this connectivity has not been well characterized in humans. However, human imaging studies have found activation to threat-related and negatively valenced stimuli in both the CeA (Costafreda et al., 2008; Fox and Shackman, 2017; Fusar-Poli et al., 2009; Lindquist et al., 2016; Sabatinelli et al., 2011; Sergerie et al., 2008) and BNST (Alvarez et al., 2011; Herrmann et al., 2016; Pedersen et al., 2016; Shackman and Fox, 2016; Somerville et al., 2010; Somerville et al., 2013). BNST and CeA activity is modulated by individual differences in anxiety during affective processing. For example, trait anxiety is associated with increased activation during threat monitoring (Somerville et al., 2010) and a blunted response to unfamiliar faces (Pedersen et al., 2017). Generalized anxiety disorder is associated with an increased BNST response to uncertainty during a gambling task (Yassa et al., 2012).

* Corresponding author.
E-mail address: walkerped@gmail.com (W.S. Pedersen).

https://doi.org/10.1016/j.neuroimage.2019.116428
Received 22 July 2019; Received in revised form 31 October 2019; Accepted 1 December 2019
Available online 3 December 2019

Similarly, the BOLD response to negatively valenced stimuli is increased by trait anxiety in fMRI activation clusters consistent with CeA (Beesdo et al., 2009; Killgore and Yurgelun-Todd, 2005; Sehlmeyer et al., 2011; Sjouwerman et al., 2018; Stein et al., 2007). Given that activity in the BNST and CeA is regulated by the reciprocal connections between these regions (Davis et al., 2010; Meloni et al., 2006), their connectivity may play a role in how they individually respond to negative and threatening stimuli. If so, BNST-CeA connectivity may shape the behavioral response to threat-related and negatively valenced stimuli in both the BNST and CeA. However, this hypothesis has received little attention in human work, and whether individual differences in BNST-CeA connectivity are related to the behavioral response to negatively valenced stimuli in humans has not yet been investigated.

1.1. BNST-CeA connectivity and negative reactivity

To investigate whether individual differences in BNST-CeA connectivity are related to the magnitude of the behavioral response to negatively valenced stimuli, we analyzed the relationship between resting-state BNST-CeA connectivity and activity of the corrugator supercilii muscle during affective image presentation in a large adult sample featuring a wide age range from the Midlife in the United States (MIDUS) study. The corrugator muscle is involved in furrowing the brow and its activity exhibits a linear relationship with affect, specifically increased activity in response to negatively valenced stimuli and reduced activity to positively valenced stimuli (Cacioppo et al., 1986; Larsen et al., 2003; Lee et al., 2009; Tan et al., 2012), and has been linked to amygdala activity (Lanteaume et al., 2007). As a point of comparison, we also tested whether differences in BNST-CeA connectivity were related to activity of the zygomaticus major, a muscle involved in smiling, in response to positive images. The zygomaticus major muscle exhibits greater activity during positive responses to pleasant stimuli but does not differentiate responses to negative and neutral stimuli (Larsen et al., 2003). As greater BNST-CeA connectivity likely reflects a combination of greater CeA excitation of the BNST, and less reciprocal inhibition between these regions, we predicted that greater BNST-CeA connectivity would be positively related to corrugator activity during presentation of negatively valenced images. We further predicted that BNST-CeA connectivity would be unrelated to both corrugator and zygomaticus activity during the presentation of positively valenced images.

1.2. BNST-CeA connectivity and negative recovery

In addition to the initial reactivity to an affective stimulus, individual differences in affective responses following stimulus offset (i.e. while recovering from the stimulus) are an important aspect of an individual's affective response profile (Schaefer et al., 2018). For example, corrugator activity during recovery from an affective image is correlated with individual differences in conscientiousness (Javaras et al., 2012) and marital stress (Lapate et al., 2014). As such, we also explored whether BNST-CeA connectivity was associated with corrugator activity during recovery from an affective image. We did so by analyzing relationships between BNST-CeA connectivity and corrugator activity during two different time windows representing early recovery (0–4 s after stimulus offset) and late recovery (4–8 s after stimulus offset). Davis et al. (2010) proposed that the CeA mediates the short-term fear response to imminent threat, while the BNST mediates the sustained anxiety response to potential or distal threat, although other researchers have challenged this distinction (Gungor and Paré, 2016; Shackman and Fox, 2016). If the CeA and BNST regulate one another's activity (Davis et al., 2010; Meloni et al., 2006), BNST-CeA connectivity may be relevant to both the immediate and more sustained response to negative stimuli. We explored whether individual differences in BNST-CeA connectivity are associated with emotional responses following the offset of an affective stimulus. We expected that greater BNST-CeA connectivity would be associated with higher corrugator activity following negative image offset.

1.3. BNST-CeA connectivity and eyeblink startle magnitude

The startle response is a quick orienting reaction to an intense stimulus, characterized by a rapid, reflexive contraction of the muscles. This response may serve to protect an organism from a blow or predator, and may contribute to readying fight or flight behaviors (Koch, 1999). Human work demonstrates that the startle response is enhanced at specific timepoints during the presentation of negatively-valenced images, and attenuated by the presentation of positively-valenced images (Bradley et al., 2006; Koch, 1999; Mauss and Robinson, 2009). Rodent research demonstrates that the CeA and BNST can both modulate the startle response (Davis, 2006). If the CeA and BNST regulate one another (Davis et al., 2010; Meloni et al., 2006), connectivity between these regions may relate to individual differences in affect-modulated startle. We tested whether individual differences in resting-state BNST-CeA connectivity was related to the magnitude of the eyeblink startle response (EBR) during and following the presentation of negative and positive images. This EBR was elicited by early (during image presentation, 2900 ms after image onset) and late acoustic probes (1900 ms after image offset). We predicted that participants with greater resting-state BNST-CeA connectivity would have larger EBR magnitudes at both time points.

1.4. BNST-CeA connectivity specificity

The amygdala is a functionally heterogeneous region (Davis and Whalen, 2001). We therefore also tested whether BNST connectivity with the basolateral amygdala (BLA) was related to the corrugator response to affective images. While not part of the extended amygdala, the BLA is thought to play a role in the extended amygdala threat response via projections to both the CeA and BNST (Davis, 1998; Davis et al., 2010). These projections are thought to relay sensory information to the extended amygdala, and likely play a role in shaping the threat response due to relevant environmental factors (Davis, 1998; Davis et al., 2010; Davis and Whalen, 2001). Thus BNST-BLA connectivity may also influence corrugator activity to negative images. However, as the BLA serves as one input of many that the extended amygdala integrates in order to coordinate the threat response, we reasoned that BNST-CeA connectivity would be a more proximal predictor of the affective response than BNST-BLA connectivity. Therefore, we predicted that higher resting-state BNST-CeA connectivity would still be associated with greater corrugator activity during negatively valenced image presentation after including BNST-BLA connectivity as a covariate. Such a finding would suggest both that BNST-CeA connectivity is distinct from BNST-BLA connectivity, and that our methods were adequate to meaningfully distinguish activity in the BLA from activity in the dorsal amygdala, which contains the CeA.

1.5. BNST-CeA connectivity, trait affect, and age

Little is known about how age may affect BNST-CeA connectivity. On average, older adults experience lower levels of negative affect, and stable levels of positive affect (Carstensen et al., 2000; Charles et al., 2001; Charles and Carstensen, 2010; Schneider, 2018). Age-related differences have also been found in both amygdala activation (Leclerc and Kensinger, 2011; Mather et al., 2004) and volume (Malykhin et al., 2008; Mu et al., 1999; Walhovd et al., 2005). Therefore, connectivity between the CeA and BNST may also be affected by age and may be a critical pathway for age to modulate affective responses. The Midlife in the United States (MIDUS) Refresher sample features a broad age range (26–76) allowing an investigation of age-related differences in BNST-CeA connectivity. We predicted that greater age would be related to lower BNST-CeA connectivity. This prediction was based on past findings showing that older adults report experiencing lower levels of negative affect (Carstensen et al., 2000; Charles et al., 2001; Charles and Carstensen, 2010; Schneider, 2018). Finally, the extended amygdala exhibits altered function in anxiety (Beesdo et al., 2009; Killgore and

Yurgelun-Todd, 2005; Pedersen et al., 2017; Sehlmeyer et al., 2011; Sjouwerman et al., 2018; Somerville et al., 2010; Stein et al., 2007; Yassa et al., 2012). We therefore predicted that greater BNST-CeA connectivity would be related to increased trait anxiety and trait negative affect.

2. Method

2.1. Participants

Data was taken from the Midlife in the United States study (MIDUS; midus.wisc.edu), a national longitudinal study of health and well-being across the lifespan. Data came from the MIDUS refresher sample, a group of participants enrolled in the MIDUS study beginning in 2011 to replenish the original MIDUS cohort. Most of these participants were recruited through random digit dialing. The MIDUS refresher sample also includes an oversampling of African American participants recruited in Milwaukee, WI, by door-to-door solicitation and stratified by gender, age and income (Ryff et al., 2017). A subset of MIDUS refresher participants who were able to travel to our laboratory were enrolled in the Neuroscience Project, which included both an MRI session and a psychophysiology session, which were completed on separate days. Resting-state data were collected for 121 participants. Thirty-nine of these participants were from the Milwaukee sample. Nineteen participants were excluded from the final analysis due to excessive motion (defined in *Imaging Analysis* below) during resting-state scanning, two were excluded because they were missing psychophysiological data, and 7 more had corrugator electromyography (EMG) data excluded because their data contained excessive noise, as determined upon visual inspection. In addition, eleven participants had zygomaticus data excluded due to excessive noise, and 14 had EBR data excluded due to having fewer than 10 valid blinks. Data from 93 participants (51 female, 42 male) were included in our primary analyses, which included corrugator and fMRI data. These participants had a mean age of 47.69 (SD = 11.7, range = 26–76). Age was not significantly different for males and females, $t(91) = -0.016$, $p = .987$. When asked their main racial origins, 62 participants endorsed White, 25 endorsed Black or African American, 2 endorsed Native American or Alaskan Native, 1 endorsed Asian, and 3 endorsed other. In addition, one participant reported being of Spanish, Hispanic or Latino descent. Additional demographic information can be found in Table 1. Analyses involving fMRI but not EMG data included 102 participants (56 female, 46 male) with a mean age of 47.33 (SD = 11.51).

2.2. Image acquisition

MRI data were collected on a 3-T MR750 General Electric scanner (GE Healthcare, Waukesha, WI) using an 8-channel head coil. High-resolution T_1-weighted whole-brain anatomical images were acquired using a BRAVO gradient-echo sequence (inversion time = 450 ms, repetition time = 8.2 ms, echo time = 3.2 ms, flip angle = 12°, field of view = 256 mm, 256 × 256 matrix, 160 axial slices).

Functional scans were acquired using a single-shot echo planar imaging sequence (240 vol, TR = 2000, TE = 20, flip angle = 60°, field of view = 220 mm, 96 × 64 matrix, 3 mm slice thickness with 1 mm gap, 40 interleaved sagittal slices, and ASSET parallel imaging with an acceleration factor of 2).

Table 1
Demographics, Neurological and Psychiatric Disorders. This table includes participants used in our primary analysis (i.e. those whose corrugator and resting-state fMRI data passed quality assurance, N = 93).

Female	54.8%
Education	
High school or less	21.5%
Some college, no degree	19.4%
Graduated college	37.6%
Advanced degree	21.5%
Marital Status	
Married	54.8%
Separated, Divorced or Windowed	23.7%
Never Married	21.5%
Self-reported neurological disorder	
Head injury	3.2%
Other (unspecified) neurological disorder	1.1%
Anxiety disorder (past 12 months)	4.3%
Depression (past 12 months)	11.8%

2.3. Region of Interest definition

BNST regions of interest (ROIs) were drawn for each individual participant in native space based on landmarks determined by consulting the Allen Institute adult human brain atlas (Ding et al., 2016), as well as prior BNST imaging studies (Avery et al., 2014; Torrisi et al., 2015). The anterior boundary was defined as the first coronal slice in which the anterior commissure could be seen intersecting the internal capsule (Fig. 1, A). In slices that were anterior to where the fornix extends below the lateral ventricle, the medial boundary was the inferior tip of the lateral ventricle (Fig. 1, B). In more posterior slices, the fornix served as the medial boundary (Fig. 1, C). Where present, the anterior commissure served as the inferior boundary. In slices where the anterior commissure did not fully span from the left to right internal capsule, the most inferior aspect of the anterior commissure when crossing the midline was used as the inferior boundary (Fig. 1, D). In the posterior direction, the ROIs were extended to where the BNST receded into the internal capsule (Torrisi et al., 2015). Left BNST ROIs had a mean size of 123 mm^3 (SD = 28 mm^3), and Right BNST ROIs had a mean size of 116 mm^3 (SD = 28 mm^3).

CeA and BLA ROIs were defined using Freesurfer (v.6.0.0, development version downloaded 5/18/2018; Fischl et al., 2002). After generating subcortical segmentations, Freesurfer's module for segmenting the nuclei of the amygdala was used to define amygdala subregions (Saygin et al., 2017). These segmentations were aligned to native space, and visually inspected. Segmentations for the basal and lateral nuclei were combined into a single mask to obtain BLA ROIs (Supplementary Fig. 1).

2.4. Imaging Analysis

Functional images were processed using FSL (FMRIB's Software Library v. 5.0.11) and AFNI (Analysis of Functional NeuroImages) version 17.3.00 (Cox, 1996). The first four volumes were discarded to allow for spins to achieve a steady state. Next the FMRI Expert Analysis Tool (FEAT) version 6.00 was used to apply motion correction (MCFLIRT; Jenkinson et al., 2002), slice timing correction, and brain extraction (Smith, 2002). Each participant's functional images were aligned to their anatomical scan using Boundary-Based Registration (Jenkinson et al., 2002; Jenkinson and Smith, 2001) and resampled to a 2 mm isotropic grid. AFNI's 3dDeconvolve program (Ward, 2002) was used to regress out six motion parameters, and signal from cerebrospinal fluid and white matter, using FAST (Zhang et al., 2001) segmentations of participant's anatomical scans which were eroded with a box kernel width of 6 mm, as well as to censor TRs with excessive motion (framewise displacement > 0.3). Participants with fewer than 120 TRs remaining after censoring were excluded. Data were bandpass filtered (0.01-0.1 Hz) and correlation maps were created by computing correlations between the mean BNST timeseries and every other voxel in the brain. This was done separately for the left and right BNST ROIs that had been resampled to a 2 mm isotropic grid. Correlation maps were then converted to Fisher's z-scores. For each correlation map (those resulting from left and right BNST seeds, respectively), the mean Fisher's z-score was extracted from the ipsilateral CeA and BLA ROIs that had been resampled to a 2 mm isotropic grid. These values served as our estimates of BNST-CeA and BNST-BLA connectivity for each hemisphere for further statistical analyses.

We also conducted whole-brain analyses investigating regions

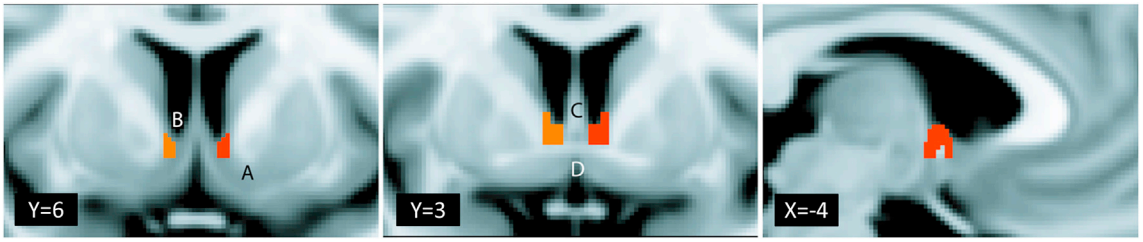

Fig. 1. BNST Region of Interest. Regions of Interest (ROIs) were drawn for each participant in native space. The example above was drawn in MNI space to highlight the landmarks used to delineate the BNST. The anterior boundary of these ROIs was defined as the first slice in which the anterior commissure can be seen intersecting the internal capsule (A). In slices that were anterior to where the fornix extends below the lateral ventricle, the medial boundary was the inferior tip of the lateral ventricle (B). In more posterior slices, the fornix served as the medial boundary (C). Where present, the superior edge anterior commissure served as the inferior boundary. In slices where the anterior commissure did not fully span from the left to right internal capsule, the most inferior aspect of the anterior commissure when crossing the midline was used as the inferior boundary (D).

exhibiting significant connectivity to the BNST (Supplementary Fig. 2), as well as regions in which connectivity with the BNST was related to the corrugator response to negative images. Methods and results from these analyses can be found in the supplemental materials.

2.5. Psychophysiology task

Participants were shown images from the International Affective Picture System (Lang et al., 2008), including 30 negative (mean IAPs valence norm = 2.9, SD =.62), 30 positive (mean valence = 7.24, SD =.44), and 30 neutral images (mean valence = 5.15, SD=.51). Images were selected based on IAPS valence norms, with positive and negative images matched on arousal (negative images: M = 5.35, SD=.54, neutral: M = 3.19, SD=.67, positive: M = 5.23, SD=.73), and all valences were matched on picture salience, luminosity, complexity, and number of pictures with social content. Trials consisted of a 1 s fixation period, followed by an image presented for 4 s, and were separated by a random 14–18 s intertrial interval. Images were surrounded by a purple or yellow border during the first 0.5 s of presentation. To ensure participants attended to the trials, they were asked to respond to the border color as quickly as possible, pressing a button with their right index finger when the border was purple and their middle finger when the border was yellow. A 50 ms, 105 dB acoustic startle probe was also included on 81 out of the 90 trials. Startle probes occurred either 2900 ms, 4400 ms or 5900 ms after picture onset, and were distributed evenly across valence conditions. Data from the probe occurring 4400 ms after stimulus onset (400 ms after image offset) were not included in analysis, as startle at this time was likely affected by prepulse inhibition (Bradley et al., 2006; Koch, 1999). Electromyographic (EMG) data were collected via three pairs of Ag–AgCl 4 mm Touchproof shielded electrodes, which were placed to measure activity from the corrugator supercilii, zygomaticus major, and inferior orbicularis oculi muscles, respectively. More information about this task can be found in van Reekum et al. (2011).

Raw EMG signals were amplified and sampled at 1000 Hz using Acknowledge software and BIOPAC hardware (BIOPAC systems, Inc., Goleta, CA). Corrugator and zygomaticus data were processed with a 60 Hz notch filter and artifacts were removed following visual inspection. Estimates of spectral power density (μV2/Hz) in the 30–200 Hz frequency band were obtained using a Fast Fourier Transform on 1 s sections (extracted through Hanning windows with 50% overlap) of artifact-free data. These estimates were log-transformed. The data were then used to create 12 1-s epochs for each valence condition, which were baseline corrected using the 1 s fixation period preceding image presentation. Data were z-scored within subject and averaged to create estimates for three 4-s time windows for each valence condition. These time windows included a reactivity time window (during the 4 s image presentation), an early recovery window (0–4 s after image offset) and a late recovery time window (4–8 s after image offset). Further information concerning the collection and processing of this data can be found in the Inter-university Consortium for Political and Social Research (ICSRP) data archive (https://doi.org/10.3886/ICPSR37094.v1).

Eyeblink reflex magnitudes were calculated as the peak integrated EMG (20–120 ms following probe onset) minus integrated EMG at onset. Trials with no perceptible eyeblink were included in the analysis with a magnitude of zero. Log-transformation was applied to normalize the data, and z-scored for each participant. Trials with invalid data were determined by visual inspection, and removed from analysis.

2.6. Self-report measures

Participants reported several demographic characteristics, as well as if they had ever suffered from a neurological disorder. Participants were also given a questionnaire (Wang et al., 2000) to determine whether they met DSM-III criteria for generalized anxiety disorder or depression within the past 12-months. Results for these variables can be found in Table 1.

Participants were also asked to complete the State-Trait Anxiety Inventory – Trait Form (STAI-X2; Spielberger et al., 1983) and the PANAS-General (Watson et al., 1988). Means for these scales were used as trait anxiety and negative affect scores, respectively.

2.7. Statistical analysis

Statistical analysis was performed in SPSS v. 24 (2016). We used linear regression to test whether greater resting-state BNST-CeA connectivity was associated with higher corrugator reactivity to the presentation of negatively valenced images. We also explored whether BNST-CeA connectivity was associated with corrugator activity during the two time windows following image presentation, including the early recovery (0–4 s after image offset) and late recovery (4–8 s after image offset) windows. We also tested associations between: 1. BNST-CeA connectivity and both the corrugator and zygomaticus response to positively valenced images, 2. The corrugator response during negative image presentation and BNST-BLA connectivity to investigate the specificity of effects for BNST-CeA connectivity, 3. BNST-CeA connectivity and EBR in response to negative and positive images during (2900 ms after image onset) and following (1900 ms after image offset) image presentation, 4. BNST-BLA with EBR during negative images, 5. age with BNST-CeA connectivity, 6. sex with BNST-CeA connectivity, and 7. BNST-CeA connectivity with self-reported trait negative affect and anxiety. All regressions involving fMRI data included average motion during the resting-state scan (mean framewise displacement) as a covariate. For significant associations, we tested whether the effect remained when controlling for age, sex and sample status (main vs. Milwaukee sample). In addition, for significant associations between BNST-CeA connectivity and the corrugator response to negative images, we tested whether this correlation was significantly different than the association between BNST-CeA connectivity and the corrugator response to positive images in the same time window using a paired correlation difference test in the R

package, "psych" (Revelle, 2018).

All reported beta-coefficients are standardized, and partial correlation (*pr*) is also reported for regressions involving more than one independent variable. Outliers were detected based on Cook's D, using a cutoff threshold of 4/(N–P) for Cook's values disconnected from the distribution. There were no cases where removing these outliers altered whether an effect was statistically significant. As a result, reported statistics include all data points, including those that met the threshold for outlier detection.

Our primary hypothesis involved the relationship between BNST-CeA connectivity and the corrugator response during negatively valenced images. As such, Holm-Bonferroni correction was applied to the two comparisons – associated with left and right BNST-CeA connectivity – involved in this hypothesis. For comparison, we also tested whether BNST-BLA connectivity was related to corrugator activity during negatively valenced images, and whether BNST-CeA connectivity was related to corrugator or zygomaticus responses to positive images. To maintain consistency, each of these comparisons were also Holm-Bonferroni corrected for two comparisons. Analyses for the early and late recovery time windows were considered more exploratory. Following the logic applied to our primary hypotheses, analyses of the association between EMG activity during these time windows and resting-state connectivity were corrected for the four comparisons (left and right hemispheres × early and late recovery time windows) within our primary valence condition (negative) and circuit of interest (BNST-CeA). Similarly, associations between EBR and BNST-CeA connectivity were corrected for four comparisons (left and right hemispheres × early and late probes). Regressions testing the relationship of BNST-CeA connectivity with age and sex were corrected for two comparisons (left and right hemispheres), while those testing the association of BNST-CeA connectivity with trait anxiety and negative affect were corrected for four comparisons (2 self-report measures × 2 hemispheres). All reported p-values are corrected, except where otherwise noted.

3. Results

3.1. Manipulation check

There was greater corrugator activity in response to negative vs. neutral images for the reactivity, $t(92) = 7.9$, $p < .001$, early recovery, $t(92) = 5.65$, $p < .001$, and late recovery time windows, $t(92) = 2.429$, $p = .017$. There was also greater corrugator activity in response to neutral vs. positive images (reactivity: $t(92) = 5.18$, $p < .001$; early recovery: $t(92) = 3.59$, $p = .001$; late recovery: $t(92) = 2.7$, $p = .007$) for all time windows. In addition, there was greater zygomaticus activity to positive vs. neutral images for the reactivity, $t(88) = 4.967$, $p < .001$, and early recovery time windows, $t(88) = 3.455$, $p = .002$, but not for the late recovery time window, $t(88) = 1.27$, $p = .207$.

There was a greater EBR during, $t(85) = 3.559$, $p = .001$, but not following, $t(85) = -0.078$, $p = .938$, negative vs. neutral image presentation. There was a greater EBR following, $t(85) = -2.927$, $p = .009$, but not during, $t(85) = .881$, $p = .381$, positive vs. neutral images. EBR was larger both during, $t(85) = 2.42$, $p = .018$, and following negative vs. positive images, $t(85) = 2.843$, $p = .011$.

There was no significant correlation between corrugator activity and the EBR during negative, $r(77) = -0.03$, $p = .795$, or positive image presentation, $r(77) = .031$, $p = .785$. There was no significant relationship between the EBR after image offset for corrugator activity during either the early (negative images: $r(77) = .016$, $p = .885$, positive images: $r(77) = -0.154$, $p = .348$) or late recovery time windows (negative images: $r(77) = -0.122$, $p = .57$, positive images: $r(77) = -0.015$, $p = .898$).

3.2. Connectivity and facial EMG during image presentation

Right BNST-CeA resting-state connectivity was related to a greater corrugator response during negative image presentation, $\beta = .311$, $pr = .314$, $t(90) = 3.14$, $p = .005$ (Fig. 2). This effect remained significant after adjusting for sex, age, sample status (i.e. whether participants came from the Milwaukee or main sample), and right BNST-BLA connectivity, $\beta = .277$, $pr = .28$, $t(86) = 2.7$, $p = .017$. Age did not significantly covary with the corrugator response in this model, $\beta = -.172$, $pr = -.177$, $t(86) = -1.67$, $p = .099$, despite a significant zero-order correlation, $\beta = -.277$, $t(91) = -2.75$, $p = .007$ (uncorrected). Right BNST-BLA connectivity was not related to the corrugator response during negative image presentation, $\beta = .053$, $pr = .054$, $t(90) = .512$, $p = 1$. Right BNST-CeA resting-state connectivity was not significantly associated with corrugator, $\beta = .022$, $pr = .022$, $t(90) = .207$, $p = 1$, or zygomaticus activity, $\beta = .029$, $pr = .029$, $t(86) = .264$, $p = .792$, during positive images. There was a trend toward right BNST-CeA connectivity having a significantly higher correlation with corrugator activity during negative than positive images but this effect did not survive correction for multiple comparisons, $t(91) = 2.15$, $p = .07$.

There was a trend toward a positive relationship between left BNST-CeA connectivity and the corrugator response during negative image presentation, $\beta = .201$, $pr = .205$, $t(90) = 1.983$, $p = .05$. Left BNST-BLA connectivity was not related to the corrugator response during negative image presentation, $\beta = -.003$, $pr = -.003$, $t(90) = -0.029$, $p = 1$ and left BNST-CeA was not related to the corrugator, $\beta = .009$, $pr = .009$, $t(90) = .082$, $p = .935$, or zygomaticus, $\beta = .101$, $pr = .101$, $t(86) = .942$, $p = .698$, response during positive image presentation. There was no significant difference in correlation between the corrugator response during negative images and BNST-CeA connectivity by hemisphere, $t(90) = .98$, $p = .33$. There was no significant difference in the correlation between left BNST-CeA and corrugator activity during negative vs. positive images, $t(91) = 1.4$, $p = .16$.

Whole-brain analysis found that there were no voxels in which resting-state connectivity with the BNST was significantly related to the corrugator response to negative images after using cluster-based correction for multiple comparisons. This was true for corrugator activity during negative image presentation, as well as for both recovery time windows.

3.3. Connectivity and facial EMG recovery time windows

BNST connectivity with the ipsilateral CeA was not associated with

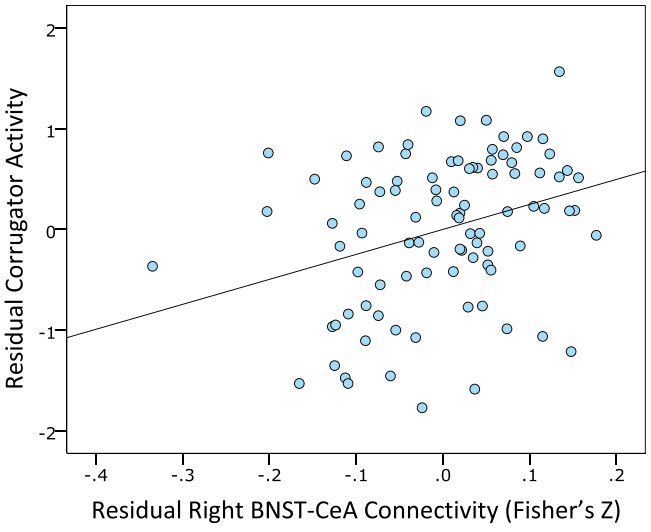

Fig. 2. Association between corrugator activity to negative stimuli and BNST-CeA functional connectivity. Partial regression plot demonstrating that greater right BNST-CeA connectivity at rest was associated with greater corrugator activity during negative image presentation, while controlling for in-scanner motion (framewise displacement). Corrugator activity was baseline-corrected, averaged over all negative picture presentations and z-scored within participant.

corrugator activity in time windows following image offset in either hemisphere. This was true for the early recovery time window (left: β = -.075, pr = -.075, $t(90)$ = -0.716, p = 1; right: β = -.002, pr = -.002, $t(90)$ = -0.02, p = 1), as well as late recovery (left: β=.051, pr = .051, $t(90)$=.488, p = 1; right: β=.104, pr = .103, $t(90)$=.987, p = 1). While there was a trend toward left BNST-BLA connectivity relating to increased late corrugator activity following negative images (p = .021, uncorrected), this effect did not survive correction for multiple comparison, β=.241, pr = .241, $t(90)$ = 2.356, p = .083. There were no other effects of BNST-BLA connectivity relating to the corrugator response following negative image presentation for any time window (all ps > .48). BNST connectivity with ipsilateral CeA was not related to corrugator (all ps > .31) or zygomaticus activity (all ps > .21) following positive image presentation for either recovery time window.

3.4. Connectivity and EBR

BNST connectivity with the ipsilateral CeA was not significantly associated with EBR magnitude during (left: β=.153, pr = .151, $t(83)$ = 1.395, p = .5; right: β=.107, $t(83)$=.973, p = .67, pr = .106) or following (left: β = -.2, $t(83)$ = -1.851, p = .27, pr = -.199; right: β=.078, $t(83)$=.713, p = .67, pr = .078) the presentation of negative images. BNST-BLA connectivity was not significantly related to EBR during negative image presentation, regardless of hemisphere (ps = 1). We did not detect a significant association between BNST-CeA connectivity and EBR during or following the presentation of positive images, for either hemisphere (ps = 1).

3.5. Connectivity, age and sex

Right BNST-CeA connectivity was negatively associated with age, β = -.293, pr = -.297, $t(99)$ = -3.098, p = .005 (Fig. 3), whereas left BNST-CeA connectivity was not, β = -.146, pr = -.149, $t(99)$ = -1.497, p = .138. BNST-BLA connectivity was not associated with age in either hemisphere (ps = 1). We did not detect a relationship between BNST-CeA connectivity and sex (left: β=.068, pr = .068, $t(99)$=.682, p = .778, right: β = -.086, pr = -.087, $t(99)$ = -0.864, p = .778). Results for age and sex were similar when participants with excessive noise in their corrugator data were excluded.

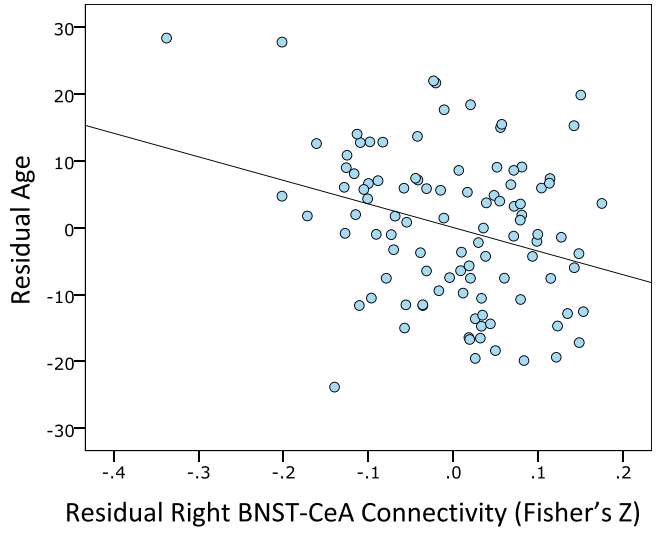

Fig. 3. Association between age and BNST-CeA functional connectivity. Partial regression plot demonstrating that greater age was associated with reduced right BNST-CeA connectivity at rest, while controlling for in-scanner motion (framewise displacement).

3.6. Connectivity, anxiety and negative affect

Participants had a mean trait anxiety score of 1.69 (SD=.463) and a mean negative affect score of 1.46 (SD=.467). There was a trend toward a relationship between right BNST-CeA connectivity and greater trait negative affect (p = .04 uncorrected), but this did not survive correction for multiple comparison, β=.205, pr = .205, $t(99)$ = 2.084, p = .16. Left BNST-CeA connectivity was not related to negative affect, β=.012, pr = .013, $t(99)$=.125, p = .978. BNST-CeA connectivity was not related to trait anxiety (left: β = -.098, pr = -.099, $t(99)$ = -0.987, p = .978; right: β=.086, pr = .086, $t(99)$=.861, p = .978).

4. Discussion

We hypothesized that greater BNST-CeA connectivity at rest would be associated with increased affective responses to negatively valenced images, as measured by increased corrugator activity and EBR magnitude. As predicted, increased right BNST-CeA connectivity was related to increased corrugator activity to negative images. While a similar pattern was observed in the left hemisphere, it did not reach statistical significance. To our knowledge, this is the first study to report a relationship between BNST-CeA connectivity and individual differences in the magnitude of a physiological response to negative emotion in humans. These results suggest that interactions between the BNST and CeA play a role in basic affective processing and that the extended amygdala is functionally relevant for negative emotional responses even in the absence of actual physical threat. Given the bidirectional connectivity that exists between the BNST and CeA, the association between greater resting-state connectivity in these regions and increased affective responses to negative images may be due to changes in connectivity in either or both directions.

While we found that resting-state BNST-CeA connectivity was related to the corrugator response to negative images, it was not related to corrugator nor zygomaticus responses to positive images. In addition, there was a trend toward a greater correlation for right BNST-CeA connectivity and corrugator activity during negative vs. positive images. Most work on the extended amygdala has focused on its role in processing negatively valenced stimuli, but evidence suggests that it also plays a role in reward related behaviors, such as food seeking and mating behaviors (Fox et al., 2015; Holland and Gallagher, 1999; Jennings et al., 2013). Reward processing in the extended amygdala may depend more heavily on interactions between the extended amygdala and other regions, such as the ventral tegmental area (Jennings et al., 2013), while BNST-CeA connectivity may be more specific to threat processes. Alternatively, it may be that negatively valenced stimuli are inherently more motivationally salient in terms of provoking withdrawal responses, than positively valenced stimuli are in provoking approach responses (Cacioppo et al., 2004). Thus, it is possible that individual differences in BNST-CeA connectivity are more closely associated with the response to negative than to positive images, due to negative stimuli being inherently more motivationally salient than positive stimuli, even when these stimuli are matched for emotional arousal.

BNST-CeA connectivity may be a more proximal cause of affective responses to negative stimuli than BNST connectivity with the BLA, which serves as one of several inputs that the extended amygdala integrates (Davis, 1998; Davis et al., 2010; Davis and Whalen, 2001). In support of this reasoning, we found that BNST-CeA connectivity continued to be related to the corrugator response to negative images after controlling for BNST-BLA connectivity. As such, BNST-CeA connectivity may be more directly relevant to behavioral measures of affective responding than BNST-BLA connectivity. This finding also suggests that our imaging methods were able to adequately distinguish BNST connectivity with the dorsal amygdala from BNST connectivity with the BLA.

While we found that right BNST-CeA connectivity was related to corrugator activity during negative image presentation, we found no

evidence that this connectivity was related to corrugator activity following image offset. In the Davis et al. (2010) model of the extended amygdala, excitation of the BNST via the CeA is critical for shifting from the initial short-term response to threat, to the more prolonged threat response, suggesting that connectivity between these regions is relevant for the late stages of affective responses to negative stimuli. However, while the Davis et al. (2010) model describes the extended amygdala response to conditions of threat, we investigated the relationship between this circuitry and the affective response to stimuli that are negatively valenced, but do not represent an actual threat. As such, different mechanisms may be at play. In addition, it may be that measuring BNST-CeA connectivity at rest provides information about the baseline sensitivity in this circuitry that is relevant to its initial reactivity to negative stimuli but is less relevant to how the affective response unfolds over time, especially following stimulus offset. Further research is needed to investigate the time course of BNST-CeA connectivity during threat processing, and its relationship to individual differences in affective behaviors and traits.

In contrast to corrugator activity, we did not detect a relationship between individual differences in BNST-CeA connectivity and the affect-modulated EBR during or following the presentation of negative images. While both affect-modulated startle and corrugator activity are measures of affective states, they likely tap into distinct processes. We found that EBR and corrugator activity during and following negative and positive images were uncorrelated. Affect-modulated startle is thought to measure priming of the fight or flight response, while corrugator activity may be a more general measure of the valence of one's current affective state (Mauss and Robinson, 2009). Thus, it is possible that individual differences in BNST-CeA connectivity at rest are more relevant to the processes giving rise the corrugator response than the startle response. In addition, past studies have found poor test-retest reliability of the EBR (Larson et al., 2000; Larson et al., 2005), especially in comparison with the reliability of corrugator emotion modulation (Lee et al., 2009), suggesting that it may have limited sensitivity as an individual differences measure. In addition, our manipulation check suggests that corrugator activity was more consistently sensitive to valence than was EBR. It may be the lack of reliability or sensitivity that contributed to the null effects observed in the relationships between the EBR and resting state BNST-CeA connectivity.

We predicted that greater BNST-CeA connectivity would be related to increased trait anxiety and negative affect. While there was a relationship between right BNST-CeA connectivity and trait negative affect, this effect did not survive correction for multiple comparisons. We found no evidence that BNST-CeA connectivity is related to trait anxiety. Fox et al. (2018) found that variation in anxious temperament was related to greater BNST-CeA connectivity in anesthetized non-human primates, while Brinkmann et al. (2018) found greater BNST-CeA connectivity during the presentation of negative and neutral images in participants reporting high trait anxiety. Further research is needed to determine the circumstances under which BNST-CeA connectivity is related to trait anxiety.

While we found that age is related to decreased BNST-CeA connectivity, the relationship between BNST-CeA connectivity and the corrugator response to negative images remained significant after adjusting for age. This set of findings suggests that the relation between BNST-CeA connectivity and the corrugator response is not simply an artifact of age affecting both variables. Given this pattern of findings, it is possible that age has some effect on the corrugator response via changes in BNST-CeA connectivity. However, given the small to medium effect sizes for both the relationship of age on BNST-CeA connectivity, and that of BNST-CeA connectivity on the corrugator response, any indirect effect is likely quite small. Reduced BNST-CeA connectivity may be one of several neural correlates of the changes in emotional responding that accompany age. Future research should further investigate the behavioral outcomes of age-related changes in BNST-CeA connectivity.

While our results demonstrate that individual differences in resting state BNST-CeA connectivity are related to the corrugator response to negative images, the correlational nature of the study makes it difficult to infer a particular mechanism for this relationship. Future studies should investigate how connectivity between these regions changes in response to affective stimuli. While our findings are consistent with past research, given the small size of the CeA and BNST, future research should also confirm our results with high-resolution imaging, to isolate signal from this circuitry with greater precision.

Our results implicate BNST-CeA connectivity in the behavioral response to unpleasant affective stimuli. This finding is consistent with rodent and non-human primate research suggesting that interactions between these regions shape the threat response via mutual regulation (Cai et al., 2012; Davis et al., 2010; Gungor and Paré, 2016; Meloni et al., 2006), and is also consistent with human work demonstrating that the BNST and dorsal amygdala respond to negatively valenced stimuli (Lebow and Chen, 2016; Shackman and Fox, 2016). This work extends these findings to humans demonstrating that intrinsic BNST-CeA connectivity is related to the magnitude of the behavioral response to negative affective events. Future work should investigate whether the onset of mood and anxiety disorders and their remittance are accompanied by changes in the function of this circuitry.

Funding

The MIDUS Refresher study was funded by the National Institute on Aging (P01-AG020166, U19-AG051426). The MIDUS Neuroscience Project data collection was supported by the Waisman Core grant from the National Institute of Child Health and Human Development (P30HD003352, PI: Albee Messing). WSP was supported by the National Institute of Mental Health (T32MH018931) and the National Center for Complementary and Integrative Health (1F32AT010101-01).

Declaration of competing interest

R.J.D. serves on the board of directors for the non-profit organization Healthy Minds Innovations. The other authors report no perceived or real conflicts of interest.

Appendix A. Supplementary data

Supplementary data to this article can be found online at https://doi.org/10.1016/j.neuroimage.2019.116428.

References

Brinkmann, L., Buff, C., Feldker, K., Neumeister, P., Heitmann, C.Y., Hofmann, D., et al., 2018. Inter-individual differences in trait anxiety shape the functional connectivity between the bed nucleus of the stria terminalis and the amygdala during brief threat processing. Neuroimage 166, 110–116. https://doi.org/10.1016/j.neuroimage.2017.10.054.

Cai, L., Bakalli, H., Rinaman, L., 2012. Yohimbine anxiogenesis in the elevated plus maze is disrupted by bilaterally disconnecting the bed nucleus of the stria terminalis from the central nucleus of the amygdala. Neuroscience 223, 200–208. Journal Article.

Oler, J.A., Tromp, D.P.M., Fox, A.S., Kovner, R., Davidson, R.J., Alexander, A.L., et al., 2017. Connectivity between the central nucleus of the amygdala and the bed nucleus of the stria terminalis in the non-human primate: neuronal tract tracing and developmental neuroimaging studies. Brain Struct. Funct. 222 (1), 21–39. https://doi.org/10.1007/s00429-016-1198-9.

Ryff, C., Almeida, D., Ayanian, J., Binkley, N., Carr, D.S., Coe, C., et al., 2017. Midlife in the United States (MIDUS refresher): Milwaukee African American sample, 2012-2013: version 4 [data set]. https://doi.org/10.3886/icpsr36722.v4.

Alvarez, R.P., Chen, G., Bodurka, J., Kaplan, R., Grillon, C., 2011. Phasic and sustained fear in humans elicits distinct patterns of brain activity. Neuroimage 55 (1), 389–400. https://doi.org/10.1016/j.neuroimage.2010.11.057.

Avery, S.N., Clauss, J.A., Winder, D.G., Woodward, N., Heckers, S., Blackford, J.U., 2014. BNST neurocircuitry in humans. Neuroimage 91 (0), 311–323. https://doi.org/10.1016/j.neuroimage.2014.01.017.

Beesdo, K., Lau, J.Y.F., Guyer, A.E., McClure-Tone, E.B., Monk, C.S., Nelson, E.E., et al., 2009. Common and distinct amygdala-function perturbations in depressed vs anxious adolescents. Arch. Gen. Psychiatr. 66 (3), 275–285. https://doi.org/10.1001/archgenpsychiatry.2008.545.

Birn, R.M., Shackman, A.J., Oler, J.A., Williams, L.E., McFarlin, D.R., Rogers, G.M., et al., 2014. Evolutionarily conserved prefrontal-amygdalar dysfunction in early-life anxiety. Mol. Psychiatry 19 (8), 915–922. https://doi.org/10.1038/mp.2014.46.

Bradley, M.M., Codispoti, M., Lang, P.J., 2006. A multi-process account of startle modulation during affective perception. Psychophysiology 43 (5), 486–497. https://doi.org/10.1111/j.1469-8986.2006.00412.x.

Cacioppo, J.T., Petty, R.E., Losch, M.E., Kim, H.S., 1986. Electromyographic activity over facial muscle regions can differentiate the valence and intensity of affective reactions. J. Personal. Soc. Psychol. 50 (2), 260–268.

Cacioppo, John T., Larsen, J.T., Smith, N.K., Berntson, G.G., 2004. The affect system. In: Manstead, A.S.R., Frijda, N., Fischer, A. (Eds.), Feelings and Emotions, pp. 223–242. https://doi.org/10.1017/CBO9780511806582.014.

Carstensen, L.L., Pasupathi, M., Mayr, U., Nesselroade, J.R., 2000. Emotional experience in everyday life across the adult life span. J. Personal. Soc. Psychol. 79 (4), 644–655.

Charles, S.T., Carstensen, L.L., 2010. Social and emotional aging. Annu. Rev. Psychol. 61 (1), 383–409. https://doi.org/10.1146/annurev.psych.093008.100448.

Charles, S.T., Reynolds, C.A., Gatz, M., 2001. Age-related differences and change in positive and negative affect over 23 years. J. Personal. Soc. Psychol. 80 (1), 136–151.

Chrousos, G.P., 2009. Stress and disorders of the stress system. Nat. Rev. Endocrinol. 5 (7), 374–381.

Costafreda, S.G., Brammer, M.J., David, A.S., Fu, C.H., 2008. Predictors of amygdala activation during the processing of emotional stimuli: a meta-analysis of 385 PET and fMRI studies. Brain Res. Rev. 58 (1), 57–70.

Cox, R.W., 1996. AFNI: software for analysis and visualization of functional magnetic resonance neuroimages. Comput. Biomed. Res. 29 (3), 162–173.

Crane, J.W., Buller, K.M., Day, T.A., 2003. Evidence that the bed nucleus of the stria terminalis contributes to the modulation of hypophysiotropic corticotropin-releasing factor cell responses to systemic interleukin-1β. J. Comp. Neurol. 467 (2), 232–242.

Davis, M., 1998. Are different parts of the extended amygdala involved in fear versus anxiety? Biol. Psychiatry 44 (12), 1239–1247. https://doi.org/10.1016/S0006-3223(98)00288-1.

Davis, M., 2006. Neural systems involved in fear and anxiety measured with fear-potentiated startle. Am. Psychol. 61 (8), 741–756. https://doi.org/10.1037/0003-066X.61.8.741.

Davis, M., Whalen, P.J., 2001. The amygdala: vigilance and emotion. Mol. Psychiatry 6 (1), 13–34. https://doi.org/10.1038/sj.mp.4000812.

Davis, M., Walker, D.L., Miles, L., Grillon, C., 2010. Phasic vs sustained fear in rats and humans: role of the extended amygdala in fear vs anxiety. Neuropsychopharmacology 35 (1), 105–135.

Ding, S.-L., Royall, J.J., Sunkin, S.M., Ng, L., Facer, B.A.C., Lesnar, P., et al., 2016. Comprehensive cellular-resolution atlas of the adult human brain: adult human brain atlas. J. Comp. Neurol. 524 (16), 3127–3481. https://doi.org/10.1002/cne.24080.

Dong, H.-W., Petrovich, G.D., Swanson, L.W., 2001. Topography of projections from amygdala to bed nuclei of the stria terminalis. Brain Res. Rev. 38 (1), 192–246.

Fischl, B., Salat, D.H., Busa, E., Albert, M., Dieterich, M., Haselgrove, C., et al., 2002. Whole brain segmentation: automated labeling of neuroanatomical structures in the human brain. Neuron 33 (3), 341–355. https://doi.org/10.1016/S0896-6273(02)00569-X.

Fox, A.S., Shackman, A.J., 2017. The central extended amygdala in fear and anxiety: closing the gap between mechanistic and neuroimaging research. Neurosci. Lett. https://doi.org/10.1016/j.neulet.2017.11.056.

Fox, A.S., Oler, J.A., Tromp, D.P.M., Fudge, J.L., Kalin, N.H., 2015. Extending the amygdala in theories of threat processing. Trends Neurosci. 38 (5), 319–329. https://doi.org/10.1016/j.tins.2015.03.002.

Fox, A.S., Oler, J.A., Birn, R.M., Shackman, A.J., Alexander, A.L., Kalin, N.H., 2018. Functional connectivity within the primate extended amygdala is heritable and associated with early-life anxious temperament. J. Neurosci. 38 (35), 7611–7621. https://doi.org/10.1523/JNEUROSCI.0102-18.2018.

Fusar-Poli, P., Placentino, A., Carletti, F., Landi, P., Abbamonte, M., 2009. Functional atlas of emotional faces processing: a voxel-based meta-analysis of 105 functional magnetic resonance imaging studies. J. Psychiatry Neurosci.: JPN 34 (6), 418.

Gungor, N.Z., Paré, D., 2016. Functional heterogeneity in the bed nucleus of the stria terminalis. J. Neurosci. 36 (31), 8038–8049. https://doi.org/10.1523/JNEUROSCI.0856-16.2016. The Official Journal of the Society for Neuroscience.

Heimer, L., Hoesen, G.W.V., Trimble, M., Zahm, D.S., 2007. Anatomy of Neuropsychiatry: the New Anatomy of the Basal Forebrain and its Implications for Neuropsychiatric Illness. Academic Press.

Herrmann, M.J., Boehme, S., Becker, M.P.I., Tupak, S.V., Guhn, A., Schmidt, B., et al., 2016. Phasic and sustained brain responses in the amygdala and the bed nucleus of the stria terminalis during threat anticipation. Hum. Brain Mapp. 37 (3), 1091–1102. https://doi.org/10.1002/hbm.23088.

Hofmann, D., Straube, T., 2019. Resting-state fMRI effective connectivity between the bed nucleus of the stria terminalis and amygdala nuclei. Hum. Brain Mapp. 0 (0) https://doi.org/10.1002/hbm.24555.

Hofmann, S.G., Ellard, K.K., Siegle, G.J., 2012. Neurobiological correlates of cognitions in fear and anxiety: a cognitive-neurobiological information-processing model. Cognit. Emot. 26 (2), 282–299.

Holland, P.C., Gallagher, M., 1999. Amygdala circuitry in attentional and representational processes. Trends Cogn. Sci. 3 (2), 65–73. https://doi.org/10.1016/S1364-6613(98)01271-6.

IBM SPSS, 2016. Statistics for Windows (Version Version 24). IMB Corp, Armonk, NY.

Javaras, K.N., Schaefer, S.M., van Reekum, C.M., Lapate, R.C., Greischar, L.L., Bachhuber, D.R., et al., 2012. Conscientiousness predicts greater recovery from negative emotion. Emotion 12 (5), 875–881. https://doi.org/10.1037/a0028105.

Jenkinson, M., Smith, S., 2001. A global optimisation method for robust affine registration of brain images. Med. Image Anal. 5 (2), 143–156.

Jenkinson, M., Bannister, P., Brady, M., Smith, S., 2002. Improved optimization for the robust and accurate linear registration and motion correction of brain images. Neuroimage 17 (2), 825–841.

Jennings, J.H., Sparta, D.R., Stamatakis, A.M., Ung, R.L., Pleil, K.E., Kash, T.L., Stuber, G.D., 2013. Distinct extended amygdala circuits for divergent motivational states. Nature 496 (7444), 224–228.

Killgore, W.D.S., Yurgelun-Todd, D.A., 2005. Social anxiety predicts amygdala activation in adolescents viewing fearful faces. Neuroreport 16 (15), 1671–1675. https://doi.org/10.1097/01.wnr.0000180143.99267.bd.

Koch, M., 1999. The neurobiology of startle. Prog. Neurobiol. 59 (2), 107–128. https://doi.org/10.1016/S0301-0082(98)00098-7.

Koob, G.F., 2008. A role for brain stress systems in addiction. Neuron 59 (1), 11–34. https://doi.org/10.1016/j.neuron.2008.06.012.

Koob, G.F., Volkow, N.D., 2016. Neurobiology of addiction: a neurocircuitry analysis. Lancet Psychiatr. 3 (8), 760–773. https://doi.org/10.1016/S2215-0366(16)00104-8.

Lang, P.J., Bradley, M.M., Cuthbert, B.N., 2008. International Affective Picture System (IAPS): Affective Ratings of Pictures and Instruction Manual (Technical Report A-8) (Journal Article).

Lanteaume, L., Khalfa, S., Régis, J., Marquis, P., Chauvel, P., Bartolomei, F., 2007. Emotion induction after direct intracerebral stimulations of human amygdala. Cerebr. Cortex 17 (6), 1307–1313. https://doi.org/10.1093/cercor/bhl041.

Lapate, R.C., van Reekum, C.M., Schaefer, S.M., Greischar, L.L., Norris, C.J., Bachhuber, D.R.W., et al., 2014. Prolonged marital stress is associated with short-lived responses to positive stimuli. Psychophysiology 51 (6), 499–509. https://doi.org/10.1111/psyp.12203.

Larsen, J.T., Norris, C.J., Cacioppo, J.T., 2003. Effects of positive and negative affect on electromyographic activity over zygomaticus major and corrugator supercilii. Psychophysiology 40 (5), 776–785. https://doi.org/10.1111/1469-8986.00078.

Larson, C.L., Ruffalo, D., Nietert, J.Y., Davidson, R.J., 2000. Temporal stability of the emotion-modulated startle response. Psychophysiology 37 (1), 92–101. https://doi.org/10.1111/1469-8986.3710092.

Larson, C.L., Ruffalo, D., Nietert, J.Y., Davidson, R.J., 2005. Stability of emotion-modulated startle during short and long picture presentation. Psychophysiology 42 (5), 604–610. https://doi.org/10.1111/j.1469-8986.2005.00345.x.

Lebow, M., Chen, A., 2016. Overshadowed by the amygdala: the bed nucleus of the stria terminalis emerges as key to psychiatric disorders. Mol. Psychiatry 21 (4), 450.

Leclerc, C.M., Kensinger, E.A., 2011. Neural processing of emotional pictures and words: a comparison of young and older adults. Dev. Neuropsychol. 36 (4), 519–538. https://doi.org/10.1080/87565641.2010.549864.

Lee, H., Shackman, A.J., Jackson, D.C., Davidson, R.J., 2009. Test-retest reliability of voluntary emotion regulation. Psychophysiology 46 (4), 874–879. https://doi.org/10.1111/j.1469-8986.2009.00830.x.

Lindquist, K.A., Satpute, A.B., Wager, T.D., Weber, J., Barrett, L.F., 2016. The brain basis of positive and negative affect: evidence from a meta-analysis of the human neuroimaging literature. Cerebr. Cortex 26 (5), 1910–1922. https://doi.org/10.1093/cercor/bhv001.

Malykhin, N.V., Bouchard, T.P., Camicioli, R., Coupland, N.J., 2008. Aging hippocampus and amygdala. Neuroreport 19 (5), 543–547. https://doi.org/10.1097/WNR.0b013e3282f8b18c.

Mather, M., Canli, T., English, T., Whitfield, S., Wais, P., Ochsner, K., et al., 2004. Amygdala responses to emotionally valenced stimuli in older and younger adults. Psychol. Sci. 15 (4), 259–263. https://doi.org/10.1111/j.0956-7976.2004.00662.x.

Mauss, I.B., Robinson, M.D., 2009. Measures of emotion: a review. Cognit. Emot. 23 (2), 209–237. https://doi.org/10.1080/02699930802204677.

Meloni, E.G., Jackson, A., Gerety, L.P., Cohen, B.M., Carlezon, W.A., 2006. Role of the bed nucleus of the stria terminalis (BST) in the expression of conditioned fear. Ann. N. Y. Acad. Sci. 1071, 538–541. https://doi.org/10.1196/annals.1364.059 (Journal Article).

Mu, Q., Xie, J., Wen, Z., Weng, Y., Shuyun, Z., 1999. A quantitative MR study of the hippocampal formation, the amygdala, and the temporal horn of the lateral ventricle in healthy subjects 40 to 90 years of age. Am. J. Neuroradiol. 20 (2), 207–211.

Oler, J.A., Birn, R.M., Patriat, R., Fox, A.S., Shelton, S.E., Burghy, C.A., et al., 2012. Evidence for coordinated functional activity within the extended amygdala of non-human and human primates. Neuroimage 61 (4), 1059–1066. https://doi.org/10.1016/j.neuroimage.2012.03.045.

Pedersen, W.S., Balderston, N.L., Miskovich, T.A., Belleau, E.L., Helmstetter, F.J., Larson, C.L., 2016. The effects of stimulus novelty and negativity on BOLD activity in the amygdala, hippocampus, and bed nucleus of the stria terminalis. Soc. Cogn. Affect. Neurosci. 12 (5), 748–757.

Pedersen, W.S., Muftuler, L.T., Larson, C.L., 2017. Disentangling the effects of novelty, valence and trait anxiety in the bed nucleus of the stria terminalis, amygdala and hippocampus with high resolution 7T fMRI. Neuroimage 156, 293–301 (Journal Article).

Revelle, W., 2018. Psych: procedures for personality and psychological research (version 1.8.12). Retrieved from. https://CRAN.R-project.org/package=psych.

Sabatinelli, D., Fortune, E.E., Li, Q., Siddiqui, A., Krafft, C., Oliver, W.T., et al., 2011. Emotional perception: meta-analyses of face and natural scene processing. Neuroimage 54 (3), 2524–2533. https://doi.org/10.1016/j.neuroimage.2010.10.011.

Sakanaka, M., Shibasaki, T., Lederis, K., 1986. Distribution and efferent projections of corticotropin-releasing factor-like immunoreactivity in the rat amygdaloid complex. Brain Res. 382 (2), 213–238. https://doi.org/10.1016/0006-8993(86)91332-6.

Saygin, Z., Kliemann, D., Iglesias, J., van der Kouwe, A.J., Boyd, E., Reuter, M., et al., 2017. High-resolution magnetic resonance imaging reveals nuclei of the human amygdala: manual segmentation to automatic atlas. Neuroimage 155, 370–382 (Journal Article).

Schaefer, S.M., van Reekum, C.M., Lapate, R.C., Heller, A.S., Grupe, D.W., Davidson, R.J., 2018. The temporal dynamics of emotional responding: implications for well-being and health from the MIDUS neuroscience project. In: Ryff, C.D., Krueger, R.F. (Eds.), The Oxford Handbook of Integrative Health Science, pp. 354–366. https://doi.org/10.1093/oxfordhb/9780190676384.013.27. S. M. Schaefer, C. M. van Reekum, R. C. Lapate, A. S. Heller, D. W. Grupe, & R. J. Davidson.

Schneider, S., 2018. Extracting response style bias from measures of positive and negative affect in aging research. J. Gerontol.: Series B 73 (1), 64–74. https://doi.org/10.1093/geronb/gbw103.

Sehlmeyer, C., Dannlowski, U., Schöning, S., Kugel, H., Pyka, M., Pfleiderer, B., et al., 2011. Neural correlates of trait anxiety in fear extinction. Psychol. Med. 41 (4), 789–798. https://doi.org/10.1017/S0033291710001248.

Sergerie, K., Chochol, C., Armony, J.L., 2008. The role of the amygdala in emotional processing: a quantitative meta-analysis of functional neuroimaging studies. Neurosci. Biobehav. Rev. 32 (4), 811–830. https://doi.org/10.1016/j.neubiorev.2007.12.002.

Shackman, A.J., Fox, A.S., 2016. Contributions of the central extended amygdala to fear and anxiety. J. Neurosci. 36 (31), 8050–8063. https://doi.org/10.1523/JNEUROSCI.0982-16.2016. The Official Journal of the Society for Neuroscience.

Sjouwerman, R., Scharfenort, R., Lonsdorf, T.B., 2018. Individual differences in fear learning: specificity to trait-anxiety beyond other measures of negative affect, and mediation via amygdala activation. BioRxiv 233528. https://doi.org/10.1101/233528.

Smith, S.M., 2002. Fast robust automated brain extraction. Hum. Brain Mapp. 17 (3), 143–155.

Somerville, L.H., Whalen, P.J., Kelley, W.M., 2010. Human bed nucleus of the stria terminalis indexes hypervigilant threat monitoring. Biol. Psychiatry 68 (5), 416–424. https://doi.org/10.1016/j.biopsych.2010.04.002.

Somerville, L.H., Wagner, D.D., Wig, G.S., Moran, J.M., Whalen, P.J., Kelley, W.M., 2013. Interactions between transient and sustained neural signals support the generation and regulation of anxious emotion. Cerebr. Cortex 23 (1), 49–60.

Spencer, S.J., Buller, K.M., Day, T.A., 2005. Medial prefrontal cortex control of the paraventricular hypothalamic nucleus response to psychological stress: possible role of the bed nucleus of the stria terminalis. J. Comp. Neurol. 481 (4), 363–376.

Spielberger, C.D., Gorsuch, R.L., Lushene, R., Vagg, P.R., Jacobs, G.A., 1983. Manual for the State-Trait Anxiety Inventory. Consulting Psychologists Press, Palo Alto, CA.

Stein, M.B., Simmons, A.N., Feinstein, J.S., Paulus, M.P., 2007. Increased amygdala and insula activation during emotion processing in anxiety-prone subjects. Am. J. Psychiatry 164 (2), 318–327.

Tan, J.-W., Walter, S., Scheck, A., Hrabal, D., Hoffmann, H., Kessler, H., Traue, H.C., 2012. Repeatability of facial electromyography (EMG) activity over corrugator supercilii and zygomaticus major on differentiating various emotions. J. Ambient Intell. Humanized Comput. 3 (1), 3–10. https://doi.org/10.1007/s12652-011-0084-9.

Torrisi, S., O'connell, K., Davis, A., Reynolds, R., Balderston, N., Fudge, J.L., et al., 2015. Resting state connectivity of the bed nucleus of the stria terminalis at ultra-high field. Hum. Brain Mapp. 36 (10), 4076–4088.

Van Reekum, C.M., Schaefer, S.M., Lapate, R.C., Norris, C.J., Greischar, L.L., Davidson, R.J., 2011. Aging is associated with positive responding to neutral information but reduced recovery from negative information. Soc. Cogn. Affect. Neurosci. 6 (2), 177–185. https://doi.org/10.1093/scan/nsq031.

Walhovd, K.B., Fjell, A.M., Reinvang, I., Lundervold, A., Dale, A.M., Eilertsen, D.E., et al., 2005. Effects of age on volumes of cortex, white matter and subcortical structures. Neurobiol. Aging 26 (9), 1261–1270. https://doi.org/10.1016/j.neurobiolaging.2005.05.020.

Wang, P.S., Berglund, P., Kessler, R.C., 2000. Recent care of common mental disorders in the United States. J. Gen. Intern. Med. 15 (5), 284–292. https://doi.org/10.1046/j.1525-1497.2000.9908044.x.

Ward, B.D., 2002. Deconvolution Analysis of fMRI Time Series Data. Biophysics Research Institute, Medical College of Wisconsin, Milwaukee, WI.

Watson, D., Clark, L.A., Tellegen, A., 1988. Development and validation of brief measures of positive and negative affect: the PANAS scales. J. Personal. Soc. Psychol. 54 (6), 1063–1070. https://doi.org/10.1037/0022-3514.54.6.1063.

Yassa, M.A., Hazlett, R.L., Stark, C.E., Hoehn-Saric, R., 2012. Functional MRI of the amygdala and bed nucleus of the stria terminalis during conditions of uncertainty in generalized anxiety disorder. J. Psychiatr. Res. 46 (8), 1045–1052. https://doi.org/10.1016/j.jpsychires.2012.04.013.

Zhang, Y., Brady, M., Smith, S., 2001. Segmentation of brain MR images through a hidden Markov random field model and the expectation-maximization algorithm. IEEE Trans. Med. Imaging 20 (1), 45–57. https://doi.org/10.1109/42.906424.